Photolytic and photocatalytic degradation of doxazosin in aqueous solution

Ivana Tartaro Bujak, Mojca Bavcon Kralj, Dmitry Kosyakov, Nikolay Ul'yanovskii, Albert Lebedev, Polonca Trebše

PII: S0048-9697(20)33652-4

DOI: https://doi.org/10.1016/j.scitotenv.2020.140131

Reference: STOTEN 140131

To appear in: *Science of the Total Environment*

Received date: 21 April 2020

Revised date: 30 May 2020

Accepted date: 9 June 2020

Please cite this article as: I.T. Bujak, M.B. Kralj, D. Kosyakov, et al., Photolytic and photocatalytic degradation of doxazosin in aqueous solution, *Science of the Total Environment* (2020), https://doi.org/10.1016/j.scitotenv.2020.140131

Photolytic and photocatalytic degradation of doxazosin in aqueous solution

Ivana Tartaro Bujak,[1] Mojca Bavcon Kralj,[2] Dmitry Kosyakov[3], Nikolay Ul'yanovskii[3], Albert Lebedev[3,4,*], Polonca Trebše[2,*]

[1]*Rudjer Bošković Institute, Division of Materials Chemistry, Zagreb, Croatia*

[2]*University of Ljubljana, Faculty of Health Sciences, Ljubljana, Slovenia*

[3]*Northern (Arctic) Federal University, Core Facility Center „Arktika“, Arkhangelsk, Russia*

[4]*Moscow State University, Department of Chemistry, Moscow, Russia*

**Corresponding authors: polonca.trebse@zf.uni-lj.si, a.lebedev@org.chem.msu.ru*

Abstract

Doxazosin (DOX), a selective alpha blocker, is widely used in medical therapy as an effective antihypertensive agent. It is a frequently prescribed drug and for this reason, environmental and ecotoxicological research is of great importance in terms of exposure and risk for both aquatic species and humans. In this study we focused on photolytic and TiO_2 photocatalytic degradation processes of doxazosin under different simulated conditions, with the emphasis on identification of degradation products. Photolytic (without TiO_2) experiments were performed in the presence and absence of oxygen, while photocatalytic degradation of doxazosin aqueous solution has been carried out under constant oxygen flow. DOX degradation was more

efficient in the TiO_2/UVA photocatalytic experiment than during photolytic processes (UVA and UVC, UVC-N_2).

LC-HRMS analyses with electrospray ionization allowed observing the formation of several major degradation products depending on the reaction conditions (presence or absence of oxygen, photocatalysis). The transformation products were identified based on exact mass measurements, isotopic distribution, and fragmentation pattern. Among them, dominated $C_{17}H_{21}N_5O_3$ and $C_{17}H_{23}N_5O_4$ (cleavage of the dioxane cycle), and $C_{23}H_{25}N_5O_7$ (hydroxylation). The detailed degradation pathway has been proposed.

Toxicity testing with V. fischeri luminescent bacteria revealed higher toxicity of samples in photolytic rather than photocatalytic experiments which might be attributed to the formation of different products.

Keywords: doxazosin, photolysis, photocatalysis, LC-MS, toxicity

1. Introduction

1. A large number of anthropogenic chemicals at trace levels are constantly releasing into the environment and their presence and implication for the environment's integrity are of special concern for the past decade. Emerging organic contaminants (EOCs) are some of those contaminants that are not commonly monitored in the environment (Stuart et al., 2012; Lebedev, 2013, Meffe et al., 2014, Richardson and Trnes, 2018). EOCs include disinfection by-products, industrials, pharmaceuticals, detergents and personal care products. The maximum permissible concentrations for some of these substances in the environment are not specified, but nevertheless even at low concentrations they affect living organisms. The number of compounds that are currently regulated by legislation is growing due to new studies related to toxicity and environmental impacts (Bavcon Kralj et al. 2007; Bielen et al. 2017; Bull et al., 2011; Jones et al., 2007, Klatte et al., 2017). This is especially the case for pharmaceutical preparations and their active ingredients used in human and veterinary medicine in large quantities for the treatment and prevention of diseases in humans and animals. Despite the fact that thousands of pharmaceuticals have been approved for use, their presence and fate in the environment has only been tested for a small fraction of them. Therefore, the need to deeper understanding the behaviour and occurrence of pharmaceuticals and their degradation products in the environment is crucial.

Due to high stability of pharmaceuticals in water and incomplete removal during conventional wastewater treatment processes (Wang et al., 2016; Santos et al., 2010) some pharmaceuticals end up in the environment, mainly in surface waters, groundwater and also in drinking water (Wang et al., 2012, der Beek et al., 2016,

Ikehataet al., 2006). In this research heterogeneous TiO_2 photocatalysis (Žabar et al. 2012; Bavcon Kralj *et al*., 2007) being a version of Advanced Oxidation Processes (AOPs), as promising method for pharmaceutical removal (Klavarioti et al. 2009; Kanakaraju 2018; Karpinska et al. 2019, Tong et al. 2011) have been applied.

Doxazosin (DOX), a selective alpha blocker, was chosen for this study due to its widespread use in medical therapy as an effective antihypertensive agent. It is frequently prescribed drug. The concentrations of DOX in raw water was found to be lower than 10 ng/L (Huerta-Fontela et al., 2011). Although this concentration is very low, DOX and its metabolites may present a potential hazard for humans and aquatic species. There are several studies dealing with stress decomposition of DOX (Ojha et al., 2003), fragmentation pathway of DOX under electron ionization conditions (El-Desawy et al. 2017) and DOX chemical behaviour under sunlight irradiation (Karpinska et al., 2019). Nevertheless, to the best of our knowledge the complete degradation scenario of DOX under TiO_2 photocatalytic conditions together with the degradation mechanism and toxicity of photoproducts have not been studied yet.

In this study we have focused on DOX photostability under different irradiating conditions in aqueous solution and identification of forming products with LC-MS/MS tool. On this basis, the degradation pathway was proposed. Additionally, the study was upgraded with the TiO_2 photocatalytic study, as one of promising AOPs method, and products identification, as well as evaluation in terms of toxicity assessment.

2. Experimental

2.1. Materials

Doxazosin mesylate (DOX), analytical standard, was provided by Sigma-Aldrich (≥ 97 %, HPLC). Aeroxide® P25 TiO_2 was provided by Sigma Aldrich. Chemicals for HPLC-DAD analyses were as follows: acetic acid glacial 100 % p.a. from Merck, ammonium acetate from Sigma-Aldrich, acetonitrile, Chromasolv for HPLC, from Sigma Aldrich Company Ltd. and double deionised water (< 18 MΩ cm) was prepared through the NANOpure water system (Barnstead, USA). Chemicals for TOC analyses were; potassium hydrogen phthalate (Nacalai Tesque Inc Kyoto, Japan), potassium nitrate (Sigma Aldrich Company), hydrochloric acid 37 % puriss. p.a. from Sigma Aldrich Company Ltd. Chemicals for ion chromatography were; sodium carbonate from Fluka, sodium bicarbonate from Fluka and Multivalent Ion chromatography Standard solution from Fluka.

2.2. Photolytic and photocatalytic studies

The experiments were conducted in a stirred cylindrical quartz reactor with a working volume of 0.1 L and an inner diameter of 40 mm. The reactor was placed in the middle of a closed cabinet allowing to use up to 12 lamps inside as a light source. In our case, two types of light sources, UVA and UVC lamps were used corresponding to 4 15 W-UVA lamps (Philips Cleo; broad maximum at 355 nm) and 4 18W-UVC lamps (Philips special, TL-D, 254 nm). The temperature was kept constant during the experiment at 28 ± 2 °C. Aqueous solutions of DOX were prepared daily in double deionised water in concentrations 10.0 ± 0.71 mg L^{-1} for photolysis and

photocatalysis. The experiments were carried out in ultrapure water to allow the identification of products formed exclusively from degradation of DOX and not from the reactions of DOX with other substances present in the environment. Photocatalytic experiments were performed by addition 4 mg of TiO_2 to 100 mL of aqueous solution of DOX and stirred for 15 minutes in dark to ensure total adsorption / desorption equilibrium of DOX onto TiO_2 surface (efficiency ± 10 %). In the case of photolytic experiments, DOX aqueous solution was irradiated for fixed periods of time under oxy- (atmospheric conditions, UVA and UVC) and anoxy- conditions (N_2 flow, UVC), while photocatalytic degradation (UVA-TiO_2) of DOX aqueous solution has been carried out under constant oxygen flow (1.5-2 mL/min) and stirring during the reaction. The aliquots of about 1.0 mL were taken periodically (0, 5, 10, 20, 30, 45, 60, 90, 120 min) and for photocatalytic measurements filtered through a membrane filter of 0.45 µm pore size. The samples were further analysed with HPLC-DAD (UV Vis), UV–Vis spectrophotometer, TOC analyzer and ion chromatography. The pH was monitored using pH meter Hanna Instruments HI 8417 and its value was around 5.9.

2.3. Analytical procedures

2.3.1. HPLC-DAD (UV-Vis) measurements and UV-Vis spectrometry

Aqueous solutions of DOX (20 µL) were analyzed by HPLC-DAD (UV-Vis) consisting of a Hewlett Packard 1100 Series chromatograph, coupled with a DAD detector operating in the UV-Vis range. The separation was achieved using Supelco C18 column (15 cm x 4.6 mm, particle size 5 µm). The column thermostat was maintained

at 25 °C and the injection volume was 20 µL. The eluents consisted of 50 % acetonitrile (A) and 50 % ammonium acetate (2.5 mM, pH 4) (B); flow rate was 0.5 mL min^{-1} and the monitored wavelengths were 247 nm and 330 nm. The retention time for DOX was 3.02 min.

The absorption spectra of DOX within irradiation time were recorded in the wavelength range of 200-800 nm with the UV-Vis spectrophotometer, Hewlett Packard 8453.

2.3.2. Identification of products by LC-HRMS/MS

All experiments were performed by liquid chromatography high-resolution mass spectrometry using HPLC system LC-30 Nexera (Shimadzu, Japan) combined with quadrupole – time-of-flight (QTOF) mass spectrometer TripleTOF 5600+ (AB Sciex, Canada). Samples for LC-HRMS/MS analysis have been concentrated 10 times in order to detect reaction products. Chromatographic separation was performed on a Nucleodur PFP column (Macherey-Nagel, Germany), 150×2 mm, particle size 1.8 µm, packed with pentafluorophenyl stationary phase, in gradient mode. Eluent composition: deionized high-purity Milli-Q water (with 0.1% formic acid) and acetonitrile (with 0.1% formic acid), gradient profile: 0-1 min 10% - acetonitrile, 1-15 min - increase in acetonitrile content up to 100%, 15-25 min - 100% acetonitrile. Flow rate - 0.25 mL min^{-1}, column temperature 40ºC, injection volume 5 µL. Ion source parameters: electrospray in positive mode (ESI+), Curtain gas pressure 30 psi, nebulising and drying gases pressure 40 psi, temperature 300ºC, ESI capillary voltage 5500 V, declustering potential 80 V. Non-targeted screening was performed in Information Dependent Acquisition (IDA) mode. Mass range in TOF-MS mode (MS):

100-1000 Da. Collision-induced dissociation (CID) was performed using collision energy (CE) 40 eV with CE spread 20 eV. Mass range in MS/MS mode: 20-1000 Da. Accurate mass measurements of the precursor and product ions allowed revealing elemental composition of all the ionic species significantly simplifying structural elucidation of the transformation products (Lebedev et al., 2013). Determination of elemental compositions of detected products was performed using their accurate masses (typical *m/z* error < 3 ppm) and isotopic distributions. Extracted ion chromatograms (XIC) for compounds with particular elemental compositions were obtained using mass window of 2.5 mDa.

2.3.3. Ion chromatography

The anions were determined according to the method described in literature (Moshoeshoe et al., 2018) on a Supelco C18 column (15 cm x 4.6 mm, particle size 5 µm). The eluents consisted of 99.8 % H_2O (A) and 0.2 % H_2SO_4 (B); with a flow rate of 1 mL min^{-1}. The injection volume was 10 µL. For quantification purposes a calibration curve for nitrate was prepared, and the r^2 value of the regression line was 0.998.

2.3.4. Statistical analysis

All experimental results were performed at least in triplicate (n ≥ 3) in order to evaluate the reproducibility of measurements the data are expressed as means ± SD.

2.3.5. Toxicity experiments

The toxicity of DOX and its degradation by-products was determined using liquid dried luminescent bacteria *V. fischeri* with system LUMIStox, Dr. Lange according to ISO 11348-2 (International Organisation for Standardisation, 1998). The toxicity endpoint was determined as reduced luminescence emission after incubation with the presence of selected compound. pH of all tested aqueous samples was adjusted to pH 7 with hydrochloric acid or sodium hydroxide in order to avoid possible adverse effects due to incorrect pH value. An aliquot of *V. fisheri* was added to each vial in two parallels and luminescence was measured immediately. Afterwards the selected sample of DOX aqueous solution was added to the vial with bacteria and thermostated to 15 ± 1 °C. The luminescence of bacteria within the sample was measured after 30 minutes of exposure. The inhibition of luminescence (with 95% confidence limit) was calculated using a computer software-supported model LUMISsoft IV. The blank test was performed with 2%, w/v sodium chloride.

3. Results and discussion

3.1. Kinetic studies - photolysis under UVC irradiation

Photolytic degradation of DOX (10 mg L^{-1}) under various irradiation conditions (UVC – presence and absence of oxygen, UVA) is presented in Figure 1. The plot $\ln(c/c_0)$ versus irradiation time in the case of UVA irradiation resulted in a linear relationship indicating that we are dealing with a pseudo first-order degradation kinetics. The

calculated disappearance rate constant for UVC photolysis was k = (5.0 x 10^{-2} ± 0.001) min^{-1} with a half life time of 13.9 min. Therefore, under UVC irradiation the concentration of DOX after 90 min reached 0.5 % of the initial concentration. The degradation was faster in the case on anoxic conditions (without oxygen) resulting in the formation of several degradation products (compounds 2 and 5, presented in Table S1 in the Supplement). In the presence of oxygen some additional products, compounds 6-9 in Table S1 were formed. On the other side, the degradation rate under UVA irradiation conditions was much slower as within 120 min only 22 % of initial doxazosin was degraded.

Figure 1

Figure 1. A disappearance curves for DOX in aqueous solution via photochemical reactions under UVC-N_2, UVC and UVA irradiation conditions.

Figure 2 illustrates the evolution of UV-Vis absorption spectra for the DOX aqueous solution upon UVC irradiation for 120 minutes. A decrease of absorbance in the whole recorded range can be clearly seen. It indicates transformation of DOX into other compounds. The photolytic spectra of DOX have shown a decrease of absorbance in the range 225-270 nm and 300-360 nm together with a slight increase of absorbance within the wavelength range 256-320 nm, which could be attributed to newly formed by-products.

Figure 2

Figure 2. UV-Vis absorbance spectra of DOX aqueous solution during 120 min of

UVC irradiation.

3.2. Kinetic study - photocatalysis

The photocatalytic degradation of the DOX aqueous solution with addition of TiO_2 resulted in the first-order degradation reaction. The observed rate constant was k = 0.127 ± 0.006 min^{-1} and a half-life time $t_{½}$ = 5.45 min (Figure 3).

Figure 3

Figure 3. The first-order disappearance curve for DOX aqueous solution via photocatalysis with TiO_2

3.3. Identification of products by LC-ESI/MS

All the products formed under different experimental conditions (photolysis and photocatalysis) and identified by LC-ESI/MS/MS are listed in Table S1. The degradation pathways are presented in Schemes 1 and 2.

Scheme 1

Scheme 1. The degradation pathway of DOX under UVC irradiation

Under UVC irradiation oxidation starts with the hydroxylation of the benzene ring attached to the dioxane moiety. One or two hydroxyls may penetrate that ring before the further reactions take place. Three pronounced peaks with close RT values

appear at the XIC chromatogram (Fig. 4) based on the ion current of m/z 468.1874 characteristic for the monohydroxylated DOX species (compounds 8). Actually, hydroxylation of the benzodioxane moiety should bring to four isomers. Maybe the fourth one forms in trace levels being hidden in the noise with RT 6.0-6.7 (Fig. 4a). Addition of nitrogen flow to the reaction mixture leads to disappearance of the isomer with RT 6.92 min (Fig. 4b)

Figure 4

Figure 4. Extracted ion chromatograms (*m/z* 468.1874) for monohydroxylated DOX (compound 8) obtained under UVC (a) UVC-N_2 (b) irradiation

Possible isomers of compound 9 contain two OH-groups in that ring. Theoretically 6 dixydroxylated isomers of that type may be formed. Since there is only one peak at the corresponding mass chromatogram, either one isomer completely dominates or the RT of these isomers are very close. The exact structure is not obvious as all four available for hydroxylation carbon atoms are activated by oxygen atoms of dioxane moiety.

The further stages of transformation of compounds 9 involve both oxidized benzene and dioxane rings, resulting in formation of products 3,4,6. It is worth mentioning that three other cycles of the initial DOX molecule remain stable as we did not detect any alternative transformation. That issue is quite interesting as dimethoxylated benzene ring should be quite reactive due to electron donating effect of the substitutes.

Intermediate product 7 demonstrates elimination of CO_2 molecule from its MH^+ ion Fig. 5a). Two possible structures reasonably rationalizing the fragmentation pattern

are demonstrated below (Fig. 5b). Based on the CID spectrum it is difficult to select the single one.

Figure 5

Figure 5 a) CID spectrum of compound 7; b) Possible structures of the intermediate UVC irradiation product No 7

Another aspect worth mentioning involves formation of two products with the reduced carbonyl group of DOX. The corresponding compounds 2 and 5 detected in trace levels in normal UVC experiment were over an order of magnitude more prominent in conditions of UVC-N_2 experiment. If compound 5 is just reduced DOX, product 2 forms due to several consecutive processes. Besides losing two original cycles (benzodioxane moiety) its both methoxy groups are hydrolyzed into hydroxyl moieties. Compound 2 is the only product with hydrolyzed methoxy groups in UVC and UVC-N_2 experiments. Possible intermediate products (5 → 2) were not detected in the UVC reaction mixture.

Scheme 2

Scheme 2: Degradation pathway of DOX during UVA-TiO_2 photocatalysis.

Two other hydrolyzed products were observed in photocatalytic conditions with TiO_2. Product 14 is reduced DOX 5 with hydrolyzed methoxy groups. It is an obvious intermediate in the process (5 → 2), although not detected in UVC conditions. Another unique hydrolyzed product (15) is the only compound, where penetration of

the first hydroxyl moiety into the molecule involves the first benzene ring, remaining benzodioxane moiety intact. Thus, that benzene ring contains three hydroxyl groups.

Actually, mass chromatogram (Fig. 6) demonstrates 6 peaks of isomeric monohydroxylated doxazosin 8 forming in the applied reaction conditions. It means that all four position of benzodioxane moiety and two position of dimethoxybenzene moiety are involved.

Figure 6

Figure 6. Extracted ion chromatogram (m/z 468.1874) for monohydroxylated DOX (compound 8) obtained under UVA-TiO_2 irradiation.

Compound 12 with carboxyl group demonstrates the cleaved dioxane ring. It transforms further into compound 10. Compound 7 (see Fig. 5b) is formed in photocatalytic conditions as well. Moreover, the closely related product 16, containing one oxygen atom less in the molecule, may be represented as an aldehyde version of compound 7. Its presence makes 7a structure containing carboxyl group more probable then the alternative 7b one (Fig. 5).

Two photocatalytic products (11 and 13) represent molecules with the oxidized saturated diazine ring. Interesting that saturated ring appears to be more reactive than the activated benzene ring with methoxy groups.

Special mentioning requires the fact that Schemes 1 and 2 represent tentative structures elucidated exclusively using CID fragmentation pattern and accurate mass measurements of the parent and product ions. Although some structures seem rather

obvious (e.g. 8 and 9) they were not confirmed by the analysis of the corresponding standards.

3.4. Ion chromatography measurements

Although pronounced DOX degradation was achieved in UVA-TiO_2 experiments, the TOC and TN analysis of samples treated via photocatalysis for 120 minutes revealed 26.97 ± 0.04 % mineralization (results not shown). Similar low mineralization has been reported for some beta blockers (Radjenović et al, 2009; De la Cruz 2013), while the case where reaction intermediates were completely mineralized to CO_2 after 240 min of irradiation was reported by (Yang et al., 2010).

Ion chromatography measurements have shown that nitrate concentration after 120 min of photocatalytic degradation reached approximately 0.5±0.1 mg L^{-1} (quantitative transformation would yield 5.66 mg L^{-1}, which is less than 10 %).

3.5. Toxicity measurements

Given the lack of data regarding the toxicity of DOX and photoproducts during photolytic and photocatalytic processes it was essential to investigate a potential risk of these compounds. The toxicity results, presented in Table 1, are as percentage of luminescence inhibition at the certain irradiation time, taking into account that this way of presenting the toxicity results is commonly adopted in the literature (Sakkas et al., 2004; Dell'Arciprete et al., 2009, 2010; Kitsiou et al., 2009). In the case of 30 min UVC photolysis in the presence of oxygen we observed certain decrease in toxicity

which rises with time and reaches the final 81.11% after 120 min of irradiation. On the contrary, in the case with irradiated samples purged with nitrogen, the toxicity slightly increases with time of irradiation and reaches the value of 77.94 % after 120 minutes of irradiation. It has to be stressed, that the toxicity of initial samples, involved in UVC experiments, was quite high (67.48 %).

Table 1

In the case of photocatalysis, the initial toxicity was lower (40.24 %) and comparable with the toxicity during irradiation with the final value of 42.1 % after 120 minutes of UVA irradiation in the presence of TiO_2. The differences in toxicity might be attributed to different mixtures effect, formed within photolytic and photocatalytic degradation processes. Several studies have performed the evaluation of toxicity of beta-blockers (atenolol and propranolol) (Yang et al., 2010), angiotensin converting enzyme (captopril) (Freitas et al. 2017) and their degradation products formed during photocatalysis and photolysis processes. Nine by-products of captotril photodegradation were nontoxic to *A. salina* and HepG2 cells. According to Toolaram et al. (2017) significant effects on bacterial luminescence of Vibrio fischeri was observed since degradation products formed during photolysis were more cytotoxic than the parent compound, atenolol. However, when comparing different antihypertensives using toxicity prediction methods (ECOSAR) propranolol is considered toxic, metoprolol is classified as harmful and atenolol as non-hazardous compound (Quaresma et al., 2018).

Anyway, an issue worth emphasizing deals with the fact that similarly to our previous studies involving snow (Polyakova et al., 2012), rain (Polyakova et al., 2018) or cloud

water (Lebedev et al. 2018) contaminants, as well as disinfection by-products (Lebedev et al., 2020) or transformation products (Zabar et al., 2016), the toxicities of the detected and tentatively identified compounds remain unknown.

4.Conclusions

The photolytic and TiO_2 photocatalytic degradation of DOX, one of the representatives of the group of antyhiperthensive drugs were performed in the present study. The obtained results indicated that DOX is relatively stable under UVA light. Only 22 % of the initial compound degraded within 120 min. On the other hand, UVC degradation was fast (after 90 min only 0.5 % of the initial DOX remained). Photocatalytic degradation with TiO_2 demonstrates pseudo first-order kinetics with relatively low level of mineralization (26,97 ± 0,04 % mineralization in 120 minutes). Analyses of inorganic ions indicated 10 % transformation of nitrogen into nitrate and no presence of nitrite ions has been observed. The formation of different sets of products in the presence or absence of oxygen with structures tentatively elucidated with LC-ESI-HRMS/MS was revealed.

Toxicity testing with V. fischeri luminescent bacteria revealed high toxicity of samples from photolytic experiments, when compared to samples treated in photocatalytic experiments which might be attributed to the formation of different products.

Knowing the fact that cardiovascular diseases are leading cause of death nowadays and that antihypertensive drugs represent frequently prescribed therapy for different cardiac disorders, the possibility to detect them in aquatic environment is very high. Therefore, additional studies focusing on degradation kinetics in different

environmental samples, identification of photoproducts, toxicity assessment of potential interactions between pharmaceutical mixtures, including antihypertensives, are extremely relevant.

5.Acknowledgements

LC-HRMS analyses were performed using instrumentation of Core Facility Center “Arktika” of Northern (Arctic) Federal University. The authors acknowledge the financial support from the Slovenian Research Agency, the research core funding No. P3-0388 (Mechanisms of health maintenance), No. J2-8162 (Closing material flows by wastewater treatment with green technologies) and bilateral scientific collaboration between Slovenia and Russia (The research of micropollutants’ path in wastewater and the reduction of environmental risk by green technologies).

6.References

Bavcon Kralj, M., Franko, M., Trebše, P., 2007. Photodegradation of organophosphorus insecticides – Investigations of products and their toxicity using gas chromatography–mass spectrometry and AChE-thermal lens spectrometric bioassay. Chemosphere 67, 99–107.

aus der Beek, T., Weber, F.A., Bergmann, A., Hickmann, S., Ebert, I., Hein, A., Küster, A., 2016. Pharmaceuticals in the environment – Global Occurrences and perspectives, Environ. Toxicol. Chem. 35, 823–835.

Bielen, A.; Šimatović, A.; Kosić-Vukšić, J.; Senta, I., Ahel, M., Babić, S., Jurina, T., González Plaza, J. J., Milaković, M., Udiković Kolić, N., 2017. Negative environmental impacts of antibiotic-contaminated effluents from pharmaceutical industries. Water Res. 126, 79–87.

Bull ,R. J., Crook J., Whittaker, M., Cotruvo, J. A., 2011. Therapeutic dose as the point of departure in assessing potential health hazards from drugs in drinking water and recycled municipal wastewater, Regul. Toxicol. Pharmacol. 60, 1–19.

De la Cruz, N., Dantas, R. F., Giménez, J., Esplugas, S., 2013. Photolysis and TiO_2 photocatalysis of the pharmaceutical propranolol: Solar and artificial light, Appl. Catal. B. 130–131, 249–256.

Dell'Arciprete, M.L., Santos-Juanes, L., Arques, A., Vercher, R.F., Amat, A.M., Furlong, J. P., Mrtire, D.O., Gonzalez, M. C., 2010. Reactivity of neonicotinoid pesticides with singlet oxygen. Catal. Today 151, 137–142.

El-Desawy, M., Zayed, M. A., Ferrag, J. 2017. Fragmentation pathway of doxazosin drug: Thermal analysis, mass spectrometry and DFT calculations and NBO analysis. J. Pharm. Appl. Chem. 3, 45–51.

Freitas, J.R.L, Jehár, F., Quintão, O., da Silva, J.C.C., Queiroz Silva, S., Aquino, SF., Afonso, R.J.C.F., 2017. Characterisation of captopril photolysis and photocatalysis

by-products in water by direct infusion, electrospray ionisation, high-resolution mass spectrometry and the assessment of their toxicities. Int. J. Environ. Anal. Chem. http://dx.doi.org/10.1080/03067319.2016.1276578

Huerta-Fontela, M, Galceran, M. T., Ventura, F., 2012. Occurence and removal of pharmaceuticals and hormones through drinking water treatment, Water Res. 45 1432–1442.

Ikehata, K., Naghashkar, N. J., El-Din, M. G., 2006. Degradation of aqueous pharmaceuticals by ozonation and advanced oxidation processes: A review," Ozone Sci. Eng. 28**,** 353–414.

Jones, O. A. H., Voulvoulis, N., Lester, J. N., 2007. Human Pharmaceuticals in Wastewater Treatment Processes, Crit. Rev. Environ. Sci. Technol. 35 (4), 401–427.

Kanakaraju, D., Glass, B. D., Oelgemöller, M., 2018. Advanced oxidation process-mediated removal of pharmaceuticals from water: A review. J. Environ. Manage. 219, 189–207.

Karpinska, J., Sokol, A., Koldys, J., Ratkiewicz, A., 2019. Studies on the Kinetics of Doxazosin Degradation in Simulated Environmental Conditions and Selected Advanced Oxidation Processes, Water. 11 (5), 1–16.

Kitsiou, V., Filippidis, N., Mantzavinos, D., Poulios, I., 2009. Heterogeneous and

homogeneous photocatalytic degradation of the insecticide imidacloprid in aqueous solutions. Appl. Catal., B 86, 27–35.

Klatte, S., Schaefer, H. K., Hempel, M., 2017. Pharmaceuticals in the environment – A short review on options to minimize the exposure of humans, animals and ecosystems. Sustain. Chem. Pharm. 5, 61–66.

Klavarioti, M., Mantzavinos, D., Kassinos, D., 2009. Removal of residual pharmaceuticals from aqueous systems by advanced oxidation processes. Environ. Int. 35 (2) 402–417.

Lebedev, A.T., 2013. Environmental Mass Spectrometry. Annu. Rev. Anal. Chem. 6, 163–189.

Lebedev, A.T., Polyakova, O.V., Mazur, D.M., Artaev, V.B., 2013. The benefits of high resolution mass spectrometry in environmental analysis. Analyst 138, 6946–6953.

Lebedev, A.T., Polyakova, O.V., Mazur, D.M., Artaev, V.B., Canet, I., Lallement, A., Vaïtilingom, M., Deguillaume, L., Delort, A.-M., 2018. Detection of semi-volatile compounds in cloud waters by GC-GC-TOFMS. Evidence of phenols and phthalates as priority pollutants. Environ. Pollut. 241, 616–625.

Lebedev, A.T., Bavcon Kralj, M., Polyakova, O.V., Detenchuk, E.A., Pokryshkin, S.A., Trebše, P., 2020. Identification of avobenzone by-products formed by various disinfectants in different swimming pool waters. Environ. Int. 137, 105495.

Meffe, R., Bustamante, I., 2014. Emerging organic contaminants in surface water and groundwater: A first overview of the situation in Italy. Sci. Total Environ. 481, 280–295.

Moshoeshoe, M.N., Obuseng V., 2018. Simultaneous determination of nitrate, nitrite and phosphate in environmental samples by high performance liquid chromatography with UV detection. S. Afr. J. Chem. 71, 79–85.

Ojha, T., Bakshi, M., Charkraborti, A. K, Singh, S. 2003. The ICH guidance in practice: Stress decomposition studies on three piperazinyl quinazoline adrenergic receptor—Blocking agents and comparison of their degradation behaviour. J. Pharm. Biomed Anal. 31, 775–783.

2. Polyakova, O.V., Mazur, D.M., Seregina, I.F., Bolshov, M.A., Lebedev, A.T., 2012. Estimation of contamination of atmosphere of Moscow in winter. J. Anal. Chem. 67, 1039–1049 (Original Russian version in Mass-spektrometria (Rus). 2012, 9, 5–15.
3.
4. Polyakova, O.V., Artaev, V.B., Lebedev, A.T., 2018. Priority and emerging pollutants in Moscow rain, Sci. Total Environ. 645, 1126–1134.

Quaresma, A. V., Sousa, B. A., Silva, K.T.S., Silva, S.Q., Werle, A.A., Afonso, R.J.C. F., 2019. Oxidative treatments for atenolol removal in water: Elucidation by mass spectrometry and toxicity evaluation of degradation products. Rapid Commun Mass Spectrom. 33, 303–313.

Radjenović, J., Sirtori, C., Petrović, M., Barceló, D., Malato, S., 2009. Solar photocatalytic degradation of persistent pharmaceuticals at pilot-scale: Kinetics and characterization of major intermediate products. App. Catal. B. 89, 255–264.

5. Richardson, S.D., Temes T.A., 2018. Water Analysis: Emerging Contaminants and Current Issues. Anal. Chem. 90, 398–428.

Sakkas, V.A., Arabatzis, I.M., Konstantinou, I.K., Dimou, A.D., Albanis, T.A., Falaras, P., 2004. Metolachlor photocatalytic degradation using TiO2 photocatalysts. Appl. Catal., B 49, 195–205.

Santos, L.H., Araújo, A. N., Fachini, A., Pena, A., Delerue-Matos, C., Montenegro, M. C., 2010. Ecotoxicological aspects related to the presence of pharmaceuticals in the aquatic environment, J. Hazard. Mater. 175, 45–95.

Stuart, M., Lapworth, D., Crane, E., Hart, A., 2012. Review of risk from potential emerging contaminants in UK groundwater,Sci. Total Environ. 416, 1–21.

Tong, L., Eichhorn, P., Pérez, S., Wang, Y., Barceló, D., 2011. Photodegradation of azithromycin in various aqueous systems under simulated and natural solar radiation: Kinetics and identification of photoproducts. Chemosphere 83, 340–348.

Toolaram, A.P., Menz, J., Rastogi, T., Leder, C., Kümmerer, K., Schneider, M., 2017. Hazard screening of photo-transformation products from pharmaceuticals: Application to selective β1-blockers atenolol and metoprolol. Sci Total Environ. 579,1769–1780.

Wang, J., Chu L., 2016. Irradiation treatment of pharmaceuticals and personal care products (PPCPs) in water and wastewater, Rad. Phys. Chem. 125**,** 56–64.

Wang, J.L., Xu, L.J., 2012. Advanced oxidation processes for wastewater treatment: formation of hydroxyl radical and application. Crit. Rev. Environ. Sci. Technol. 42**,** 251–325.

Yang, H., An T., Li G., Song, W., Cooper, W.J., Luo, H., Guo, X., 2010. Photocatalytic degradation kinetics and mechanism of environmental pharmaceuticals in aqueous suspension of TiO_2: A case of β-blockers. J. Hazard. Mater. 179, 834–839.

Zabar, R., Bavcon Kralj, M., Komel, T., Fabjan J., Trebše P., 2012. Photocatalytic degradation with immobilised TiO_2 of three selected neonicotinoid insecticides: imidacloprid, thiamethoxam and clothianidin. Chemosphere. 89, 293–301.

Zabar, R., Sarakha, M., Lebedev, A.T., Polyakova, O.V., Trebse, P., 2016. Photochemical fate and photocatalysis of 3,5,6-trichloro-2-pyridinol, degradation product of chlorpyrifos. Chemosphere 144, 615-620.

Table 1. Bioluminescence inhibition for V. fischeri of DOX in distilled water at 0 and 120 minutes under different reaction conditions

Sample	% of inhibition
DOX/H_2O	67.48
120 min UVC	81.11
120 min UVC-N_2	77.94
TiO_2-DOX/H_2O	40.24
120 min UVA-TiO_2	42.1

CRediT author statement

Albert Lebedev: Methodology, Software, Validation, Resources, Writing - Review & Editing, Supervision, Funding acquisition; **Mojca Bavcon Kralj**: Methodology, Visualization, Supervision; **Ivana Tartaro Bujak:** Investigation; **Dmitry Kosyakov**: Formal analysis; **Nikolay Uljanovskii**: Formal analysis; **Polonca Trebše**: Conceptualization; Methodology, Supervision; Resources, Writing - Review & Editing, Project administration, Funding acquisition

Declaration of competing interest

The authors declare that they have no known competing financial interests or personal relationships that could have appeared to influence the work reported in this paper.

Highlights:

- Degradation of doxazosin was more effective under photocatalytic conditions than photolytic;
- LC-MS/MS allowed identifying a number of doxazosin transformation products;
- Toxicity assessment was done for photolytic and photocatalytic degradation;
- Photocatalysis was evaluated in terms of nitrate formation;

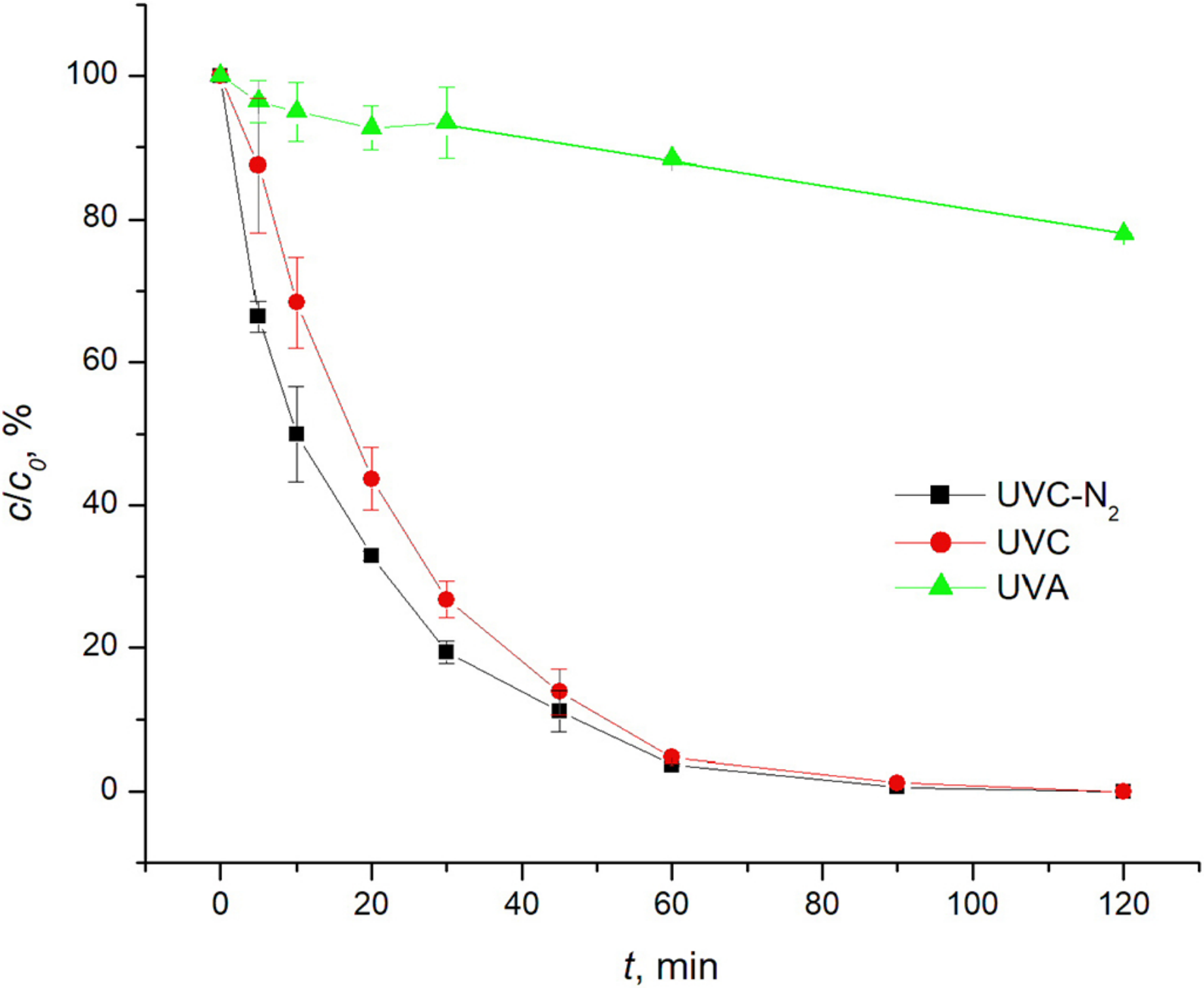

Figure 1

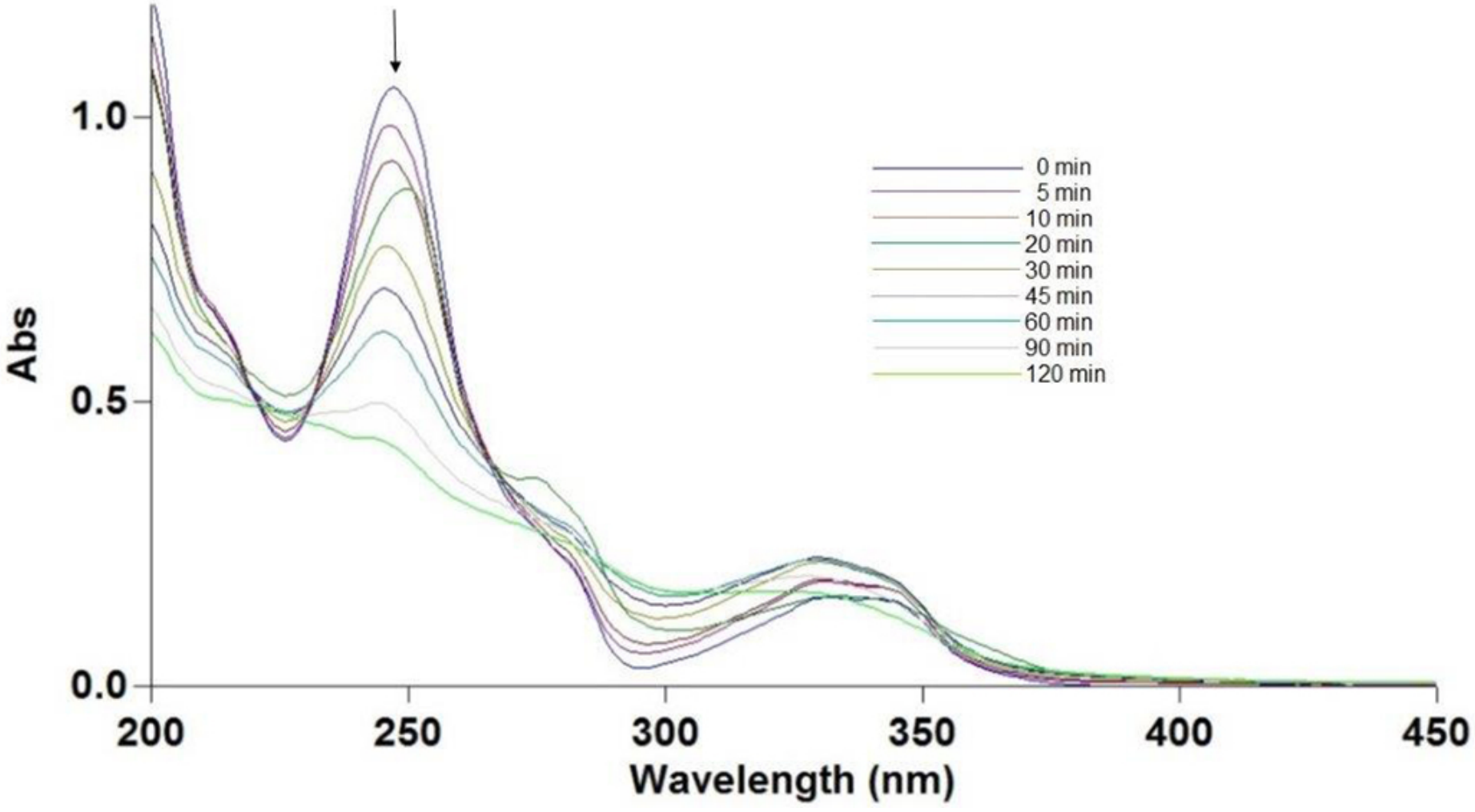
1.0
0.5
0.0
Abs
200
250
300
350
400
450
Wavelength (nm)
0 min
5 min
10 min
20 min
30 min
45 min
60 min
90 min
120 min

Figure 2

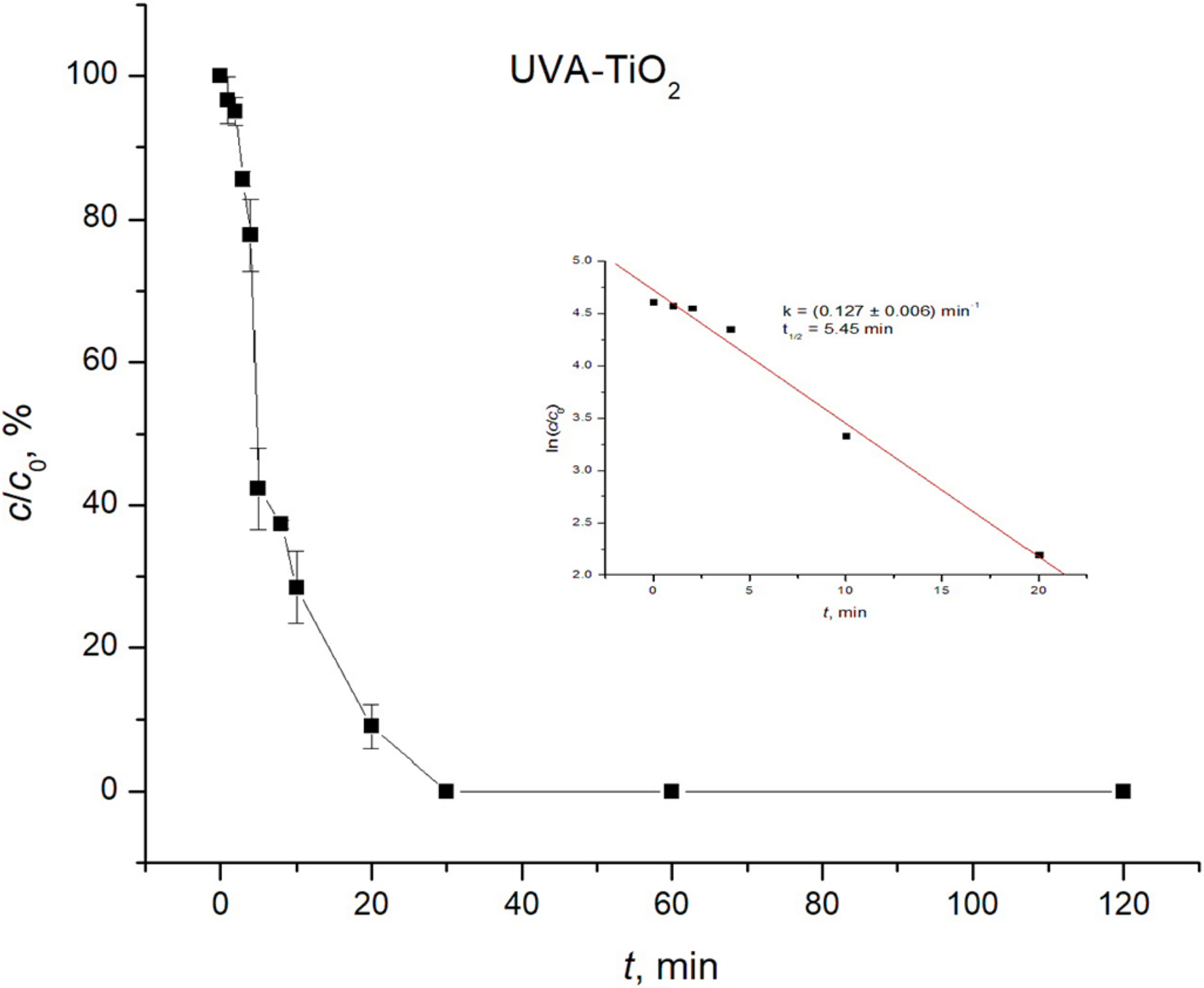
UVA-TiO2
c/c0, %
t, min
100
80
60
40
20
0
0
20
40
60
80
100
120
ln(c/c0)
k = (0.127 ± 0.006) min-1
t1/2 = 5.45 min
5.0
4.5
4.0
3.5
3.0
2.5
2.0
0
5
10
15
20
t, min

Figure 3

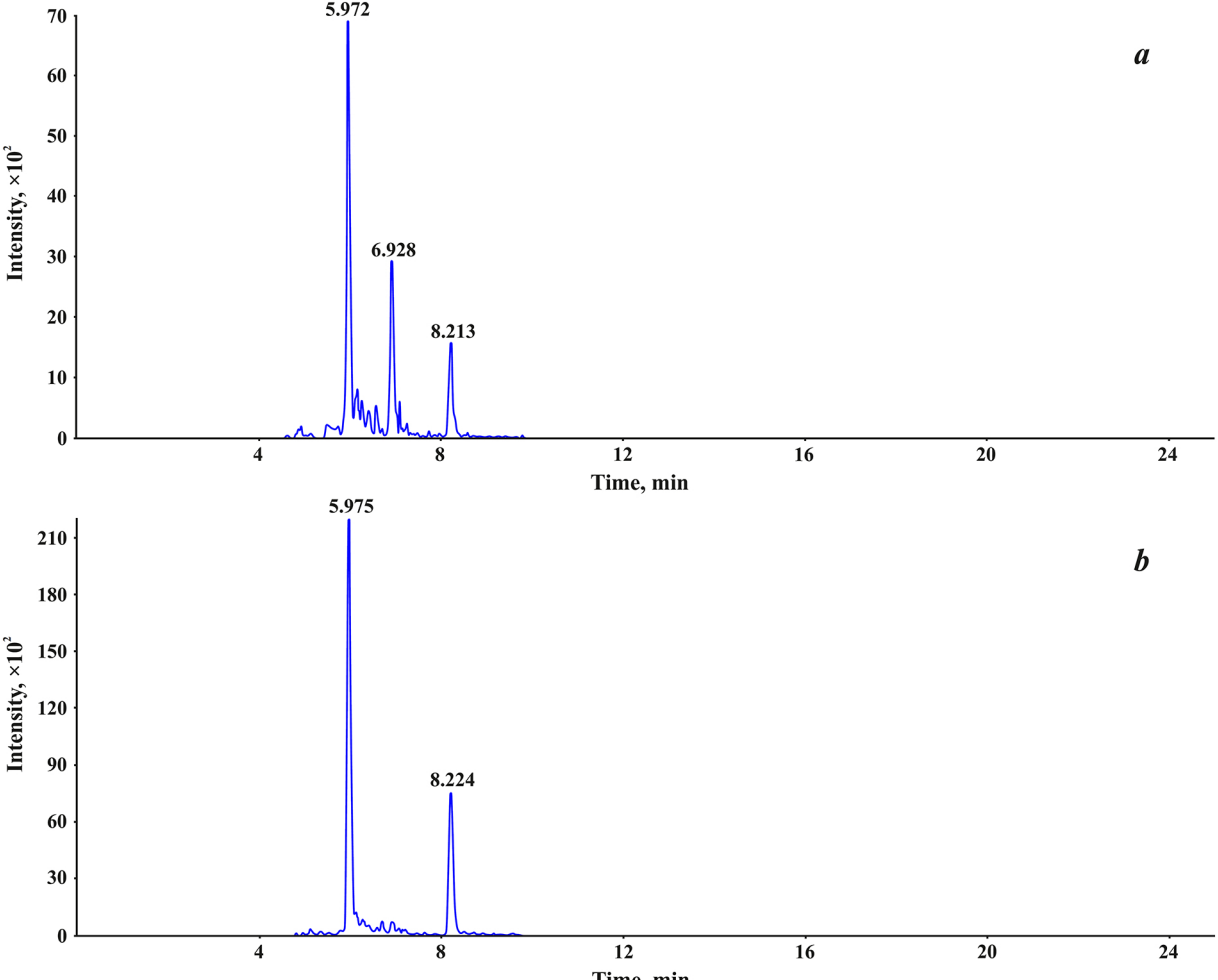
a
5.972
6.928
8.213
Intensity, ×10²
Time, min
b
5.975
8.224
Intensity, ×10²
Time, min

Figure 4

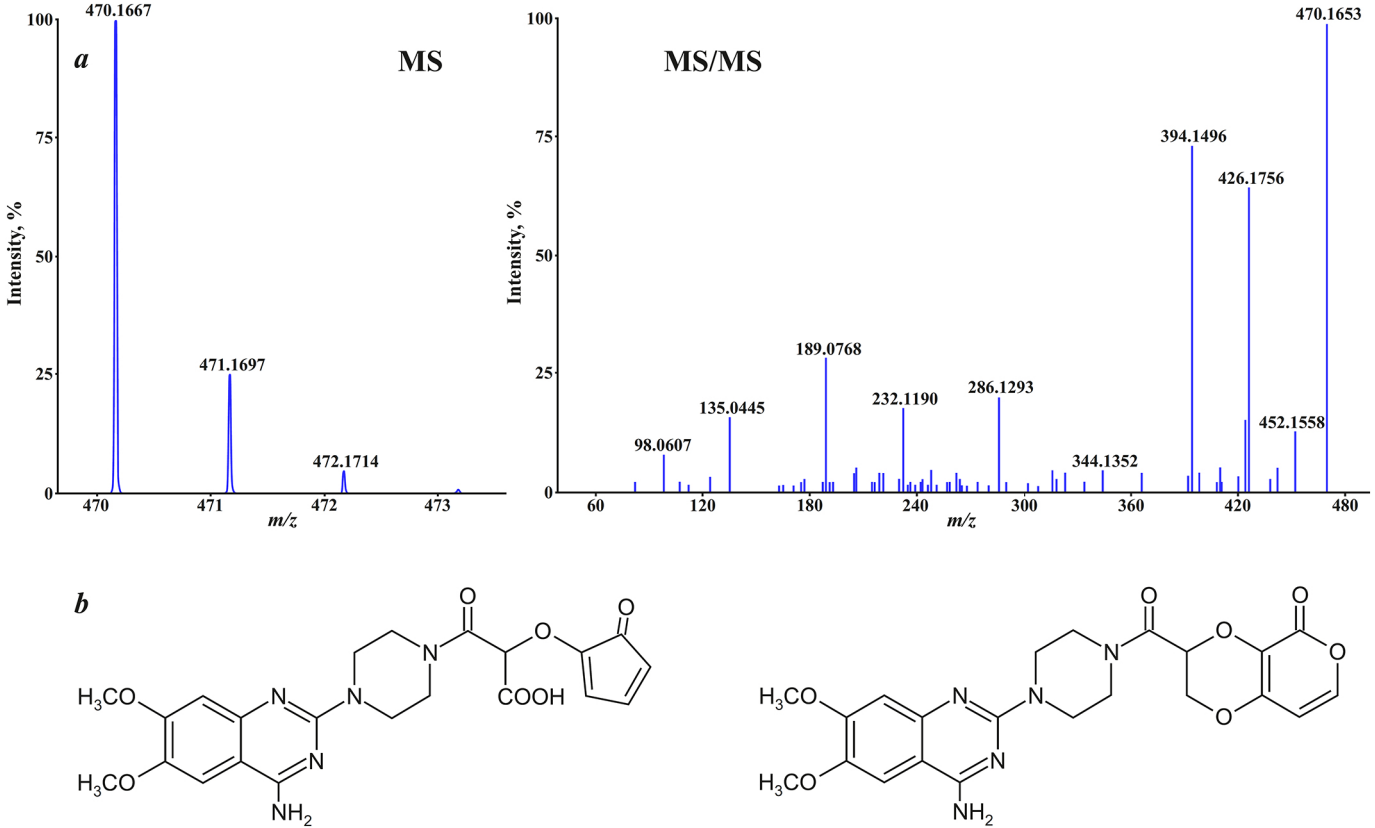
a
MS
470.1667
471.1697
472.1714
Intensity, %
m/z
MS/MS
470.1653
394.1496
426.1756
189.0768
232.1190
286.1293
135.0445
98.0607
452.1558
344.1352
b
H3CO
H3CO
NH2
COOH

Figure 5

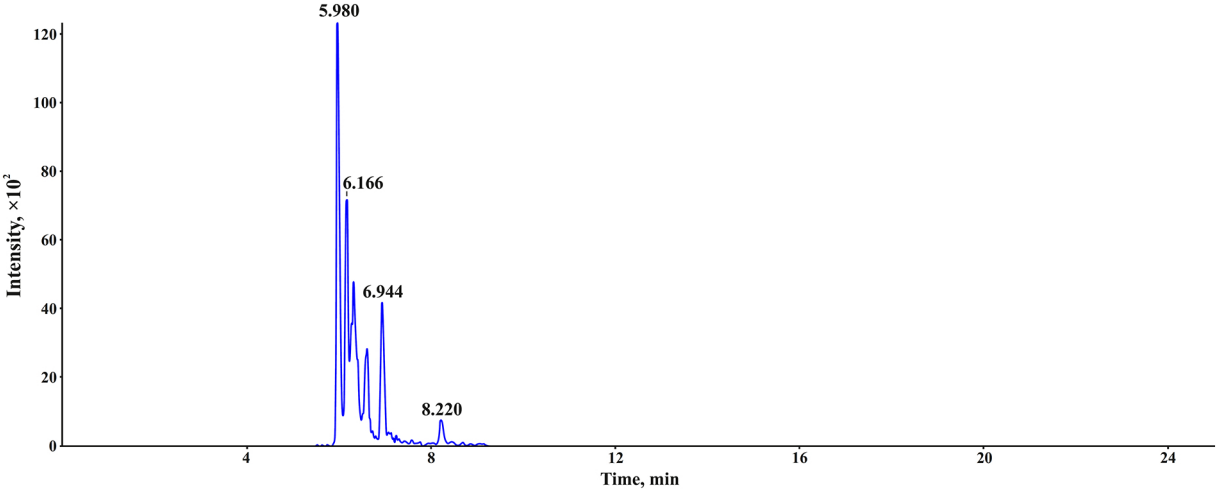
5.980
6.166
6.944
8.220
Intensity, ×10²
Time, min
0
20
40
60
80
100
120
4
8
12
16
20
24

Figure 6